HHS Public Access

Author manuscript

Biomaterials. Author manuscript; available in PMC 2016 November 01.

Published in final edited form as:

Biomaterials. 2015 November ; 68: 54–66. doi:10.1016/j.biomaterials.2015.07.053.

Nanoparticle Delivery of CDDO-Me Remodels the Tumor Microenvironment and Enhances Vaccine Therapy for Melanoma

Yan Zhao[a,b], **Meirong Huo**[a,c], **Zhenghong Xu**[a], **Yuhua Wang**[a,*], and **Leaf Huang**[a,*]

[a]Division of Molecular Pharmaceutics, Center for Nanotechnology in Drug Delivery, Eshelman School of Pharmacy, University of North Carolina at Chapel Hill, Chapel Hill, North Carolina 27599, United States

[b]Department of Pharmaceutics, School of Pharmacy, China Medical University, Shenyang 110122, China

[c]State Key Laboratory of Natural Medicines, Department of Pharmaceutics, China Pharmaceutical University, Nanjing 210009, China

Abstract

Lipid-calcium-phosphate nanoparticle (NP) delivery of Trp2 peptide vaccine is one of the most effective vaccine strategies against melanoma. However, due to the immunosuppressive microenvironment in the tumor, the achievement of potent immune responses remains a major challenge. NP delivery systems provide an opportunity to deliver chemotherapy agent to modulate the tumor microenvironment (TME) and improve the vaccine activity. Anti-inflammatory triterpenoid methyl-2-cyano-3,12-dioxooleana-1,9(11)-dien-28-oate (CDDO-Me) is a broad spectrum inhibitor of several signaling pathways that are important in both cancer cells and cells in the TME. Intravenous delivery of CDDO-Me using poly-lactic-glycolic-acid NP combination with subcutaneous Trp2 vaccine resulted in an increase of antitumor efficacy and apoptotic tumor tissue than Trp2 vaccine alone in B16F10 melanoma. There was a significant decrease of both Treg cells and MDSCs and a concomitant increase in the cytotoxic T-lymphocyte infiltration in TEM of the vaccinated animals. Also, CDDO-Me remodeled the tumor associated fibroblasts, collagen and vessel in TME, meanwhile, enhanced the Fas signaling pathway which could sensitize the tumor cells for cytotoxic T lymphocyte mediated killing. The combination of systemic induction of antigen-specific immune response using Trp2 nanovaccine and targeted modification of the TME with the NP delivered CDDO-Me offers a powerful combination therapy for melanoma.

Keywords

Nanoparticle; CDDO-Me; Peptide vaccine; Tumor microenvironment; Melanoma

*Address correspondence to either alwong1982@gmail.com or leafh@unc.edu.

1. Introduction

Cancer immunotherapy has become one of the most promising strategies in cancer therapy. A number of antitumor vaccines have been tested for their ability to induce tumor-specific immune response and antitumor treatment *in vivo* [1–3]. Moreover, several clinical trials have recently demonstrated promising therapeutic potential for cancer vaccine [4–6]. Current cancer immunotherapy includes diverse strategies that such as activating innate and adaptive immune system responses by neutralizing the inhibitory and suppressive mechanisms in the tumor [7,8]. During tumor growth progression, tumor-induced immunosuppression is a major obstacle for immunotherapeutic strategies that avoid immune recognition and elimination [9,10]. Therefore, development of an effective treatment to break the immunosuppression in the tumor microenvironment (TME) remains a major challenge for cancer immunotherapy.

Previous studies in our lab used a potent mannose-modified LCP nanoparticle (NP)-based vaccine containing both tumor-specific antigen and adjuvant, to activate the dendritic cells (DC). It also generated a strong *in vivo* cytotoxic T lymphocyte (CTL) response against the poorly immunogenic self-antigen tyrosinase-related protein 2 (Trp2) peptide. This ultimately resulted in a potent anti-tumor immune response against the Trp2 expressing melanoma [11]. Previous studies also indicated that Trp2 LCP vaccination results in potent growth inhibition of a B16F10 melanoma model in both early (4 days after tumor inoculation) and late (13 days after tumor inoculation) stages [12]. Early vaccination on day 4 exhibited significant tumor growth inhibition; whereas late vaccination was much less potent, despite of the fact that the systematic CTL response was the same. Most likely, immune suppression gained along with tumor progression compromised the efficiency of the immunotherapy.

The antitumor effects of immunotherapy can be enhanced by its combination with chemotherapeutic agents that can modulate the immune response [13–16]. Therefore, we investigated the potential benefits of combining antigen-specific LCP-based vaccination with chemotherapeutic agents targeting the TME with the hopes of improving the anti-tumor effect in an advanced B16F10 melanoma model. Anti-inflammatory triterpenoid methyl-2-cyano-3,12-dioxooleana-1,9(11)-dien-28-oate (CDDO-Me) is a synthetic oleanane triterpenoid, an effective agent for solid cancer prevention and treatment, with some well-understood anti-carcinogenic mechanisms [17,18]. CDDO-Me has strong anti-proliferative and pro-apoptotic activities in diverse types of tumor cell lines [19–22]. The anticancer mechanisms of CDDO-Me include induction of apoptosis and modulation of several signal transduction pathways, such as PI3K/Akt/mTOR, MAPK (Erk1/2), NF-κB, TGF-β/Smad and Nrf2 signaling pathways [23–25]. Furthermore, CDDO-Me can also block the immune suppressive function of myeloid-derived suppressor cells (MDSCs) and improve the immune response to cancer [26]. The accumulation of immunosuppressive regulatory T-cells (Treg) and MDSCs within the TME is a major obstacle to effective antitumor immunotherapies. Therefore, we investigated the delivery of CDDO-Me targeting the TME for an effective treatment against advanced stage tumors. CDDO-Im, an analog of CDDO-Me, has been shown to improve the activity of a DNA vaccine and prevent recurrence in breast cancer when delivered to the TME [27]. We hypothesize that targeted delivery of CDDO-Me to the tumor using poly-lactic-glycolic-acid (PLGA) NP will result in a

modulation of the TME and enhance the activity of a peptide vaccine against advanced melanoma (scheme 1).

2. Materials and methods

2.1. Materials

1,2-Dioleoyl-3-trimethylammonium-propane chloride salt (DOTAP), 1,2-distearoryl-*sn*-glycero-3-phosphoethanolamine-*N*-[methoxy(polyethyleneglycol-2000)] ammonium salt (DSPE-PEG) and dioleoylphosphatydic acid (DOPA) were purchased from Avanti Polar Lipids (Alabaster, AL, USA). Cholesterol was purchased from Sigma-Aldrich (St. Louis, MO, USA). DSPE-PEG-Mannose was synthesized using DSPE-PEG-NHS (NOF, Shibuya-ku, Tokyo) and 4-Amino phenyl α-D-mannopyranoside (Sigma-Aldrich, St. Louis, MO) in our laboratory as previously reported and the structure was confirmed using ^{1}H NMR [11]. PLGA was purchased from DURECT (Pelham, AL, USA), PLGA-PEG and PLGA-PEG-MBA were synthesized using PLGA, $mPEG_{3000}$-NH_2·HCl and $tBOC\text{-}PEG_{3500}$-NH_2·HCl (JenKem Technology, Allen, TX) in our lab as described previously and the structure was confirmed using ^{1}H NMR [47]. H-2K^{b} restricted peptides Trp2 (SVYDFFVWL, MW 1175), OVA (SIINFEKL, MW 1773) and modified Trp2 peptide, p-Trp2 (pSpSSSVYDFFVWL, MW 1626) were purchased from Peptide 2.0 (Chantilly, VA, USA). CpG ODN 1826 (5′-TCCATGACGTTCCTGACGTT-3′) was obtained from Sigma-Aldrich (St. Louis, MO, USA). CDDO-Me was purchased from Selleckchem (Houston, TX, USA).

2.2. Cell line and mice

Murine melanoma cell line B16F10 was obtained from American Type Culture Collection (ATCC) and cultured with DMEM supplemented with 10% fetal bovine serum, 100 U/mL penicillin and 100 μg/mL streptomycin (Invitrogen, Carlsbad, CA). Female C57BL/6 mice with the age of 6 to 8 weeks were purchased from the National Cancer Institute (Bethesda, MD, USA). All animal procedures were carried out under protocols approved by the Institutional Animal Care and Use Committees at the University of North Carolina at Chapel Hill.

2.3. Preparation of PLGA-based CDDO-Me NP

The solvent displacement method was employed for the formation of CDDO-Me loaded PLGA NP (CDDO-Me NP). Briefly, 0.2 mg of CDDO-Me and 4 mg of polymers, including PLGA, PLGA-PEG and PLGA-PEG-MBA, were dissolved in 0.4 mL of tetrahydrofuran (THF), NP were formed by adding the drug polymer solution dropwise into 4 mL of stirring water at room temperature. The suspension was allowed to stir uncovered for 6 h at room temperature to evaporate the organic solvent. The CDDO-Me NP was purified by ultrafiltration (50,000 NMWL, Millipore, Billerica, MA) at 4000 *g* for 15 min. The CDDO-Me NP was then re-suspended, washed with water and collected with 5% glucose. The CDDO-Me NP was observed by TEM, particle size distributions and zeta potential were determined using a Malvern Zetasizer Nano ZS. Loaded concentrations of CDDO-Me were measured using a UV spectrophotometer (Beckman Coulter, Atlanta, GA). EE and DL were calculated according to the formulas:

$$EE = \frac{\text{Amounts of drug in NPs}}{\text{Total amount of drug}} \times 100\%$$

$$DL = \frac{\text{Amounts of drug in NPs}}{\text{Total weight of NPs}} \times 100\%$$

2.4. In vitro release of CDDO-Me NP

To study the release of CDDO-Me from PLGA NP, dialysis devices were used with phosphate buffered saline (PBS) at 37°C with pH 7.4 and 6.8. In order to establish the sink condition, 0.25% Tween-80 was added in the PBS. CDDO-Me NP with a final concentration of 200 μg/mL was placed into a dialysis tube with a molecular weight cutoff of 3000 Da and dialyzed against 14 mL PBS in a thermo-controlled shaker with a stirring speed of 150 *rpm*. Samples of 140 μL were withdrawn at predetermined time intervals and centrifuged at 15000 *g* for 15 min. The concentration of CDDO-Me was determined by UV spectrophotometer (Beckman Coulter, Atlanta, GA). The samples taken for measurement were replaced with fresh media and the cumulative amount of drug released into the media at each time point was calculated as the percentage of total drug released to the initial amount of the drug. The *in vitro* releases were performed in triplicate for both pH.

2.5. Preparation of LCP-based p-Trp2 vaccine NP

The LCP-based p-Trp2 vaccine was prepared by water-in-oil micro-emulsion technique as previously described [12]. Briefly, 600 μL $CaCl_2$ (2.5 M) containing p-Trp2 peptide and CpG ODN was dispersed in 20 mL Cyclohexane/Igepal CO-520 (71:29, v/v) solution to form a well-dispersed Ca phase. Meanwhile, 600 μL Na_2HPO_4 (12.5 mM, pH 9.0) and 200 μL DOPA (20 mM) were dispersed in another 20 mL oil phase to obtain the phosphate phase. After the above micro-emulsion phases were stirred 15 min separately, they were mixed and stirred for another 30 min. Subsequently, 40 mL ethanol was added to break the micro-emulsion. After that, CaP cores were collected by centrifugation (10,000 *g* × 20 min) and washed with ethanol three times. The pellets were dissolved in chloroform and mixed with 100 μL DOTAP (20 mM), 100 μL cholesterol (20 mM), 20 μL DSPE-PEG-2000 (20 mM) and 20 μL DSPE-PEG-mannose (20 mM). After evaporating the chloroform, LCP vaccine particles were dispersed in 100 μL of 5% glucose. The morphologies of p-Trp2 LCP NP were observed by transmission electron microscopy (JEOL 100CX II TEM, JEOL, Japan). Particle size and zeta potential were measured by a Malvern Zetasizer Nano ZS (Malvern, Worcestershire, UK).

2.6. Tumor growth inhibition

To determine the effects of the Vac and CDDO-Me on tumor growth, C57BL/6 mice were *s.c.* inoculated with 2×10^5 B16F10 cells on their flank on day 0. On days 13, the Vac was *s.c.* injected into the contralateral side of the inoculation site for the vaccine only and combination therapy group. Starting on day 13, the mice were treated with *i.v.* injections of CDDO-Me NP or intraperitoneal (*i.p.*) injections of CDDO-Me free every other day for a

total of three injections at a dose of 5 mg/kg. Thereafter, tumor size was measured every day using digital calipers (Thermo Fisher Scientific, Pittsburgh, PA) and tumor volume was calculated as: Tumor volume (mm^3)=0.5×length×$width^2$. Body weight was also monitored. After completion of the therapeutic experiment on days 18, mice were humanely sacrificed and tumor tissue and major organs were collected for further experiments.

2.7. TUNEL assay

For detection of apoptotic cells in tumor tissues, the TUNEL assay was carried out using a DeadEnd Fluorometric TUNEL System (Promega, Madison, WI) according to the manufactures instructions. Mice were sacrificed at the designated time points and tumor tissue were quickly harvested from the body and immersed in 10% formalin for 48 h. The fixed tumor tissues were then paraffin-embedded and 5 μm thick histological sections were prepared (obtained from the UNC Histopathology Core Facility). Cell nuclei that were fluorescently stained with green were defined as TUNEL-positive nuclei. The sections were stained by 4,6-diaminidino-2-phenyl-indole (DAPI) Vectashield (Vector laboratories, Burlingame, CA) and covered with a coverslip. TUNEL-positive nuclei were monitored using a fluorescence microscope (Nikon, Tokyo, Japan) at 100× magnification. Three randomly selected microscopic fields were quantitatively analyzed on Image J software.

2.8. Safety evaluation

Tumor-bearing mice were injected and sacrificed at the designated time points and major organs were quickly harvested from the body and immersed in 10% formalin for 48 h. The fixed organs were then paraffin-embedded and 5 μm thick histological sections were prepared (obtained from the UNC Histopathology Core Facility). The paraffin sections were mounted onto slides and stained with hematoxylin and eosin. The morphological features of the tissues were observed under a light microscope for analysis of tissue injuries. Meanwhile, the blood samples were collected and assessed for hepatic and renal function, included aspartate aminotransferase (AST), alanine amino transferase (ALT), blood urea nitrogen (BUN), and creatinine by UNC facility.

2.9. PLGA NP biodistribution assay

C57BL/6 mice bearing B16F10 tumors were *i.v.* administered with a single dose of 1 μCi ^{3}H-labeled PLGA NP and were sacrificed 24 h post-intravenous administration. Tissue samples were first digested by Tissue Solubilizer (Amersham Biosciences Corp. NJ, USA) overnight at room temperature and then with 4 mL scintillation cocktail (Thermo Fisher Scientific Inc., MA, USA). The samples were then assayed using a liquid scintillation counter (Beckman coulter LS6500). The percentage of the injected dose (% ID) in the tissue was calculated. All tests were done in triplicate.

2.10.PLGA NP cellular uptake assay

C57BL/6 mice were *s.c.* inoculated with 2×10^5 B16F10 cells on their flanks on day 0. On days 13, the mice were *i.v.* injected with a single dose of PLGA NP labeled with a lipophilic dye, 1,1′-dioctadecyl-3,3,3′,3′- tetramethylindocarbocyanine perchlorate (DiI), at a dose of 0.5 mg/kg and were sacrificed 24 h post-intravenous administration. The DiI-loaded PLGA

NP was prepared as described for CDDO-Me-loaded PLGA NP in section 2.3. Tumor tissue was harvested and digested with collagenase A and hyaluronidase at 37°C for 40 min. After lysis of the red blood cells, the dissociated cells were dispersed with 1 mL PBS. The immune lymphocytes (5×10^6 /mL) were stained with fluorescein-conjugated CD11b antibody (BD Biosciences, San Jose, CA). Immunocyte uptake of DiI-loaded PLGA NP was detected by flow cytometry. All tests were done in triplicate.

2.11. Flow cytometry assay

Tumor-infiltrating and splenocyte immune lymphocytes were analyzed by flow cytometry. In brief, tumor and spleen tissues were harvested and digested with collagenase A and hyaluronidase at 37°C for 40 min. After lysis of the red blood cells (RBCs), the dissociated cells were dispersed with 1 mL of PBS. For intracellular cytokine staining, the cells from the tumor and spleen tissue were penetrated with 0.1% triton-100 for 15 min. The immune lymphocytes (5×10^6/mL) were stained with the following fluorescein-conjugated antibodies: FITC-conjugated anti-mouse CD8a, FITC-conjugated anti-mouse CD4, PE-conjugated anti-mouse FOXP3, FITC-conjugated anti-mouse CD11b, and PE-conjugated anti-mouse Gr-1 (BD, New South Wales, Australia). Flow cytometry was performed in quintuplicate for each group. Analysis was performed on a FACSCalibur flow cytometer and analyzed using Cell Quest software (BD Biosciences, San Jose, CA).

2.12. Immunofluorescence

Tissue section slides were deparaffinized, antigen retrieved, permeabilized and blocked with 1% bovine serum albumin (BSA) at room temperature for 1 h. Primary antibodies conjugated with fluorophores (BD, Franklin Lakes, NJ) were incubated overnight at 4°C and nuclei were counterstained with DAPI (Vector Laboratories Inc, Burlingame, CA). All commercial binding reagents were diluted according to the manufacturer's recommendation. Images were taken using fluorescence microscopy (Nikon, Tokyo, Japan). Three randomly selected microscopic fields were quantitatively analyzed on Image J software.

2.13. In vivo cytotoxic T lymphocyte (CTL) response

The *in vivo* CTL assay was performed according to the previous protocol [12]. In brief, splenocytes from naïve C57BL/6 mice were collected and loaded with either 10 μM Trp2 or Ova peptides in complete media at 37°C for 1 h. Both loaded cell populations were stained with 2 μM PKH-26 (Sigma-Aldrich, St. Louis, MO) following the manufacturer's protocol. Then, the Trp2 peptide-pulsed and Ova peptide-pulsed cells were labeled with 4 μM and 0.4 μM CFSE, respectively. Equal amount of $CFSE^{high}$ (Trp2 pulsed cells) and $CFSE^{low}$ (Ova pulsed cells) were mixed and *i.v.* injected into the untreated and treated mice. Eighteen hours later, splenocytes were collected from these treated mice and subjected to flow cytometry analysis. The number of $CFSE^{high}$ and $CFSE^{low}$ was calculated and the *in vivo* Trp2 specific lysis percentage was enumerated according to a published equation. The *in vivo* CTL was performed in quintuplicate for each group.

$$\%specific\ lysis=\frac{(\mathrm{Ova}\times \mathrm{x}-\mathrm{Trp}2)}{\mathrm{Ova}\times \mathrm{x}}\times 100\%$$

where $x=\frac{\mathrm{Trp2}}{\mathrm{Ova}}$ *from naive mice*

2.14. Quantitative real-time PCR assay

Total RNA was extracted from tissue samples by the RNeasy kit (Qiagen, Valencia, CA) and cDNA was reverse-transcribed by SuperScript First-Strand Synthesis System for RT-PCR (Invitrogen, Grand Island, NY). Amplification was conducted with SsoAdvanced Universal Probes Supermix (Bio-rad, Hercules, CA), mouse-specific primers and 100 ng of cDNA. All the mouse-specific primers for RT-PCR reactions are listed in Table 1 (Life technologies, Grand Island, NY). GAPDH was used as an endogenous control. The RT-PCR was performed in quintuplicates for each group. The reactions were conducted using a 7500 Real-Timer PCR System, and the data were analyzed with the 7500 Software.

2.15. Masson trichrome staining

For detection of collagen in tumor tissues, the Masson Trichrome assay was carried out. Paraffin-embedded tumor sections were deparaffinized and rehydrated. The slides were then stained using a Masson Trichrome kit (Sigma-Aldrich, St Louis, MO, USA) according to manufacture instructions. Images were taken using light microscopy (Nikon, Tokyo, Japan). Three randomly selected microscopic fields were quantitatively analyzed on Image J software.

2.16. Western blot analysis

Tumor tissues were collected and proteins were extracted in radioimmunoprecipitation assay (RIPA) lysis buffer with a cocktail of proteinase inhibitors (Sigma-Aldrich, St. Louis, MO) by tissue homogenization and sonication. Total protein concentration was measured using the BCA protein assay kit (Thermo, Rockford, IL) following the manufacturer's instruction. Protein extracts were diluted in 4× sample buffer with reducing reagent and heated at 95°C for 5 min. After separation by NuPAGE 4–12% Bis-Tris protein Gels (Invitrogen, Grand Island, NY), proteins were transferred to an Immobilon-P transfer membrane (Millipore, Billerica, MA) by electrophoresis. Membranes were blocked with 1% casein blocker (Bio-Rad, Hercules, CA) for 1 h at room temperature and probed with the indicated primary antibodies Fas (Abcam, Cambridge, MA), PARP and GAPDH (Santa Cruz biotechnology, Dallas, TX) overnight at 4°C and the horseradish peroxidase- conjugated secondary antibody for 1 h at room temperature. Signals were detected using the Pierce ECL Western Blotting Substrate (Thermo, Rockford, IL). Western blot was performed in triplicate for each group and the optical density of each protein band was analyzed with Image J software.

2.17. Statistical analysis

Data were analyzed statistically using a two-tailed Student's *t*-test by comparison with the control group unless otherwise specified with markings. A p value less than 0.05 was considered statistically significant.

3. Results and discussion

3.1. CDDO-Me is encapsulated into PLGA NP for systemic administration

Nanoparticle based drug delivery systems are powerful approach to targeted deliver water-insoluble therapeutics to the tumor. Therefore, hydrophobic CDDO-Me was encapsulated into PLGA NP so that high bioavailability could be achieved in the tumor after systemic administration. To enhance the tumor uptake of NP, p-methoxybenzylamide (MBA) was used as a targeting ligand. MBA is an analog of anisamide which binds with the sigma receptors over-expressed in many murine and human epithelial tumor cells including melanoma. CDDO-Me was formulated in PLGA NP using the well-established solvent displacement method. The encapsulation efficiency (EE), drug loading (DL), size and the polydispersity index (PDI) of the CDDO-Me NP are shown in Figure S1. In summary, the EE and DL increased with the decreasing ratio of PLGA and PLGA-PEG in the polymer mix. We chose the ratio of PLGA to PLGA-PEG 2:8 and 4% (drug/excipient ratio) CDDO-Me feed to prepare the optimized PLGA NP. The EE and DL for this formulation was 61.4 ± 3.8% and 2.9 ± 0.2%, respectively (Figure S1C). The size for the CDDO-Me NP was varied from 60–100 nm determined by TEM (Figure 1A) and 120 nm by dynamic light scattering (Figure S1D) with a surface charge of −25 mV. The release of CDDO-Me from the PLGA NP exhibited a similar release rate ($T_{1/2}$ = 36 h and 42 h) in pH 7.4 and 6.8 PBS, respectively. No burst drug release was observed (Figure S1E).

As was published, LCP NP is lipid-coated, PEG-stabilized calcium phosphate nano-precipitate fabricated in a reverse microemulsion system. During the formation of precipitates, small or macromolecules with phosphate groups such as gemcitabine monophosphate, siRNAs and pDNA can be efficiently encapsulated in the NP [28–31]. The high PEG density on LCP surface significantly increased the *in vivo* colloidal stability of the NP and thus improved pharmacokinetic and pharmacodynamic profiles of the therapeutics. In order to enhance the encapsulation of hydrophobic Trp2 peptide in the LCP NP, two phosphorylated serines were added to the N-terminal of the peptide sequence without compromising the antigenic activities [11]. Phosphorylated Trp2 were thus loaded into LCP NP with CpG oligonucleotide (ODN) as an adjuvant [12]. The LCP NP was surface-functionalized with mannose to target the mannose receptor which is highly expressed in antigen presenting cells such as dendritic cells as well as macrophages [11]. The EE of p-Trp2 peptide and CpG ODN in the LCP NP was about 50% and 40%, respectively. The final LCP NP was about 30 nm in diameter as determined by TEM (Figure 1B), while hydrodynamic size of LCP is 50 nm in diameter determined by dynamic light scattering with surface charge of 15 mV.

3.2. CDDO-Me delivered by PLGA NP boosted the tumor specific immune response elicited by LCP vaccine

The anti-tumor activity of mono- or combo therapy of LCP vaccine (Vac) and CDDO-Me were evaluated in the B16F10 melanoma syngeneic animal model. B16F10 bearing C57BL/6 mice received subcutaneous (*s.c.*) Vac at relatively late stage (13 days post tumor inoculation) when there was a strong suppressive tumor microenvironment [12]. CDDO-Me were simultaneously administered to the animals in an attempt to reverse the local immune

suppression and enhanced the vaccine efficacy. Vac alone had elicited only a partial tumor growth inhibition. The combination of Vac and CDDO-Me NP (5 mg/kg) achieved a temporary tumor growth arrest for the highly aggressive tumor, although CDDO-Me NP alone showed minimal, if any, anti-tumor activity (Figure 2A and 2B). To show if nano mediated delivery was important, CDDO-Me free was also administered (*i.p.*) in combination with Vac. It was less efficacious than the combination therapy when CDDO-Me was delivered using PLGA NP (Figure S2).

TUNEL assay on the tumor tissues collected from the endpoint of the studies revealed a high percent of apoptotic cells (60%) in the tumor that received the combination therapy (Figure 2C and 2D). In comparison, Vac or CDDO-Me NP alone only induced 30% or 15% apoptotic cell, respectively. In addition, Vac+CDDO-Me free (*i.p.*) also showed significant tumor cell apoptosis, but it was less than Vac+CDDO-Me NP administration (38.1 ± 3.8 %, $p < 0.01$) (Figure S3).

In addition, we further investigated the toxicity of Vac and CDDO-Me. No decrease in body weight was observed in any of the groups, indicating that there was no apparent toxicity associated with the treatments (Figure S4). The H&E staining results of the toxicological assay in the tumor bearing mice showed that major organs including heart, liver, spleen, lungs and kidneys did not display any significant changes in morphology for separate or combinatory treatment groups (Figure S5). The hepatic and renal function data indicated that the liver functional parameters aspartate aminotransferase (AST) level in the mouse was over the normal range due to the existence of the tumor (Table S1). Various treatments did not reduce or increase the liver toxicity in the mouse model.

3.3. PLGA NP efficiently delivered CDDO-Me to the tumor associated immune cells

As the intention of the study was to deliver CDDO-Me to the tumor as an immune-modulating agent to remodel the tumor immunity, we proceeded to examine if the drug was accessible to the tumor associated immune cells. An explicit profiling of PLGA NP distribution was undoubtedly the prerequisite information to address this question.

The tissue biodistribution of PLGA NPs in the tumor-bearing mice was determined using ^{3}H-labeled PLGA NP. Trace amount of ^{3}H-labelled cholesteryl hexadecyl ether was added to the preparation of PLGA NP. This radioactive lipid serves as a stable marker for labeling NPs by hydrophobic interactions [32]. Twenty-four hours post *i.v.* injection, 3.2 ± 0.9 % ID/g of the PLGA NP accumulated in the tumor tissue (Figure 3A). This correlates to the distribution of drug distribution assuming the drugs are evenly encapsulated in the NPs.

As the tumor growth inhibition study suggested, the anti-tumor effect of combo therapy might stem from the functional modulation of tumor infiltrating leukocytes by CDDO-Me delivered using PLGA NP. To validate the hypothesis, we explored the microscale distribution of PLGA NP in tumor tissue to confirm if the CDDO-Me loaded NP would affect that population. PLGA NP was labelled with DiI and single cell suspension from tumor was subject to flow cytometry analysis. The data demonstrated that around 60% of the cells in the tumor were accessible by PLGA NPs after single injection (Figure 3B). A further analysis indicated that around 67% CD11b+ cells took up PLGA NPs (Figure 3B). In mice,

the CD11b antigen is expressed on monocyte, macrophage and myeloid-derived suppressor cells (MDSCs). Out of these cells, the M2-phenotype macrophages and MDSCs express cytokines and molecules that suppress the local immunity and pose barrier to immune therapy [33–36]. To our surprise, the choice of PLGA NP as carrier led to efficient delivery of immune modulating agents to these critical immune suppressive cells in the tumor.

3.4. CDDO-Me delivered by PLGA-NP reduced suppressive immune cell populations, which subsequently enhanced tumor specific CTL in the tumor microenvironment

PLGA NP could efficiently deliver CDDO-Me to the immunosuppressive cells in the tumor. Therefore, the populations of immune regulatory cells including MDSCs and regulatory T (Treg) cells, as well as effector CD8+ cytotoxic T cells were examined after treatment. Treg cells are immune regulator which suppresses a broad spectrum of cell types including CD4+CD8+ T cells, macrophages, DCs and NK cells via distinct mechanisms [37–39]. MDSCs are a heterogeneous population of myeloid derived cells that have features such as myeloid origin, immature statues and the capacity to inhibit innate and adaptive immune response [40]. Both Treg cells and MDSCs contribute to the T cell exhaustion [41, 42] and are associated with poor prognosis in numerous tumor types [43]. Immunofluorescence and flow cytometry has been used to quantify the specific cellular population. The results (Figure 4) demonstrated an increase percent of MDSCs and Treg cells in the tumor microenvironment after vaccination. This correlated with a moderate increase of CTL in the tumor (Figure 4C and 4F) and suggested a resistance mechanism that counteracted the CTL response elicited by the vaccine. However, CDDO-Me treatment drastically reduced the MDSCs and Treg cells counts to the level even lower than the untreated mice. This removal of suppressive cells led to the increased CTL infiltration (Figure 4D, 4E and 4F), which could account for the remarkable tumor inhibition activity.

An *in vivo* CTL assay was performed to evaluate the activity of antigen specific CD8+ killer T cells in the context of CDDO-Me treatment. As our previous studies indicated, the CTL activity elicited by vaccine was independent of mice status [12], but the killer efficiency was profoundly affected by the immune microenvironment. Spleen is one of the major lymphoid tissues that harbor many MDSCs and Treg cells, therefore CTL killing efficiency could be affected by existence of these suppressor cells. Although a large portion of the injected PLGA accumulated into the spleen (Figure 3A), there were hardly any changes in the cell populations (Figure. S6). The discrepancy of suppressive cell elimination efficiency between tumor and spleen suggested that the CDDO-Me did not kill the immune cells in the tumor. Instead, it affected the recruitment and infiltration of tumor associated immune cells by reshaping the tumor microenvironment. Similar results were reported by Nagaraj et al [26], which showed that anti-inflammatory triterpenoid blocks immune suppressive function of MDSCs and improves immune response in cancer. The *in vivo* CTL results demonstrated the killing efficiency of antigen specific CD8+ cells was much higher in the presence of CDDO-Me (Figure 5). Our study has shown the PLGA NP delivered CDDO-Me could reduce suppressor cells and enhance CD8+ T cell infiltration in the tumor. The CTL functional assay suggested another mechanism for combo therapy that CDDO-Me could indirectly boost CD8+ T cell killing efficiency by blocking the suppressor cell activity. After all, the augmentation of CTL activity was largely attributed to the high delivery efficiency to the

immune cells mediated by PLGA. It was also noteworthy that CDDO-Me treatment did not compromise the T cell activity (Figure 5), although it was generally considered an anti-inflammatory agents.

3.5. CDDO-Me delivered to immune suppressive cells and altered the cytokine expression profiles

Tumor associated immune-suppressive cells secret cytokines and chemokines to shape the tumor immune microenvironment [44]. Increased CD8+ infiltration and enhanced CTL killing efficiency both indirectly reflected the pharmacological activities of CDDO-Me on the suppressive cells. Cytokines are the direct messengers that linked the suppressive cells and T cells. Therefore, we examined the expression levels of cytokines after treatment using RT-PCR analysis. Cytokines are generally divided into two categories based on their pathogenic roles in contribution to tumorigenesis. Pro-inflammatory mediators, which are usually secreted by classical M1 macrophages that promote Th1 immune responses and antagonize the suppressive immune cells, are termed M1 cytokines (IL2, IL12a and IFN-γ). In contrast, cytokines associated with suppressive M2 macrophages and MDSCs which promote Th2 immune responses and suppress acquired immune response are termed M2 cytokines (CCL2, IL10, IL6, TNF-α and TGF-β). The results indicated that CDDO-Me delivered to macrophages and MDSCs significantly reduced M2 cytokines as well as M1 cytokines in the tumor (Figure 6). Such immune modulation, although insufficient by itself to inhibit tumor growth, greatly facilitated the action of the Vac. Apparently, this was the most important mechanism by which CDDO-Me PLGA NP enhanced the Vac effect.

3.6. CDDO-Me remodeled the TME to augment vaccine activity

Secretion of cytokines by cancer cells and stromal cells in the tumor tissue alters the local TME to support drug resistance, immunologic escape, tumor recurrence, invasion and metastasis [45]. In the TME, tumor associated fibroblasts (TAF) aid the tumor in immune modulation by impeding antitumor T cell function. The effect of the Vac and CDDO-Me NP on TAF was investigated by staining for α-smooth muscle actin (SMA), a marker for TAF. The result showed that Vac or CDDO-Me NP could significantly reduce the amount of TAF (Figure 7), which is in consistent with the report that CDDO-Me can inhibit TGF-β induced myofibroblast differentiation *in vitro* [46]. While CDDO-Me NP and Vac alone groups partially attenuated the amount of α-SMA-positive cells, the combinatory treatment of Vac +CDDO-Me NP further reduced the fibroblast population in the tumor tissue to 20.0 ± 7.0 % ($p < 0.01$) (Figure 7). Thus, the combinatory treatment of Vac+CDDO-Me NP not only affected tumor cells but also depleted TAF. Similarly, the combined treatment also brought about a significant decrease in the stroma content of the tumor tissue. We used Masson Trichrome assay to study the collagen content and the morphology in the treated tumors (Figure 8). B16F10 melanoma does not develop extensive stroma structure compared to other solid tumors [47, 48]. Stroma revealed by the collagen staining showed thin and elongated fibrous structures in the untreated tumor (blue staining indicated by arrows in Figure 8). CDDO-Me NP treatment diminished the stroma to only about 19.2±6.2% of the untreated control ($p < 0.01$), demonstrating a major effect of the drug on the TME. The collagen content further decreased to only about 4.5±1.1% ($p < 0.01$) when combined with Vac. The hypoxic tumor environment results in an abnormal blood vessel network, which

allows metastatic tumor cells to escape and strongly prevents infiltration of anti-cancer immunity and drug penetration to the tumor mass [49]. Regulation of the abnormal tumor vessel phenotype leading to normalized vasculature can restore a proper immune response in the TME [50]. Thus, we also examined the vessel content and distribution in the tumor by immunofluorescence for CD31, a vessel marker (Figure 9). Unlike the stroma, vessels were abundant and randomly distributed in the untreated tumor. Either Vac or CDDO-Me NP alone significantly reduced the vessel content to 33.3 ± 7.7 % and 30.5 ± 7.1 % of the untreated control, respectively ($p < 0.01$). The combination treatment further decreased the vessel content to 14.7 ± 3.8 % of the control. Thus, we conclude that CDDO-Me NP had a strong down-regulation effect on the TME which is likely to significantly modulate the immunosuppression in the tumor.

3.7. Augmentation of the therapeutic efficacy of the Vac and CDDO-Me NP through the Fas signaling pathway

So far, we have investigated the pharmacological effects of CDDO-Me NP delivered to the immune suppressive cells, a minor but critical population in the tumor. We would also like to study the CDDO-Me NP effects on tumor cell populations, as the majority of the cells were cancer cells according to the flow cytometry data (Figure 3B). In addition to the classical perforin/granzyme pathway for CTL activity, Fas mediated lytic pathway also contributes to the killing of the target cells [51]. Fas is a membrane receptor which transduces signal that leads to cell apoptosis. It was reported that low dose cytotoxic drugs increased Fas expression on tumor cells, thereby sensitizing the cancer cell to CTL activity [52]. Similar phenomenon was confirmed in CDDO-Me treated B16F10 cells *in vitro* (data not shown). The western blot analysis of the tumor lysate demonstrated that CDDO-Me NP treatment slightly upregulated Fas expression, which led to downstream cleavage of poly ADP ribose polymerase (PARP), an apoptotic marker (Figure 10). On the other hand, Fas expression was also elevated in Vac-treated mice which was probably induced by IFN-γ and TNF-α (Figure 6) that were associated with acquired CTL response [53]. Although both single treatments slightly sensitized the cells to CTL activity by the expression levels of Fas, the combination treatment surprisingly showed a synergistic effect. The cause of this synergism, however, requires further investigation. In the combination treatment, CDDO-Me NP showed a general anti-inflammatory effect, reducing the levels of both M1 and M2 macrophage-related cytokines including IFN-γ and TNF-α (Figure 6). Considering the fact that CDDO-Me NP only slightly increased the Fas expression and the fact that suppressed IFN-γ and TNF-α expression could not induced Fas (Figure 6), other mechanisms might be also involved in the chemoimmunotherapy which boosted the efficacy of each other. After all, the combo therapy engineered the tumor immunity, enhanced the acquired CTL response and sensitized the tumor cells to CTL-mediated lysis.

4. Conclusion

We have demonstrated that an immune-modulating agent CDDO-Me can be efficiently delivered to the tumor-associated suppressive immune cells in advanced melanoma using PLGA NP. Approximately 67% of CD11b+ cells, mostly macrophages and MDSCs, were accessible by PLGA NP after single injection. The delivery of CDDO-Me NP to those

suppressive cells efficiently altered the cytokine expression profiles. This could subsequently reduce the recruitment of immunosuppressive cells, changed the stromal structure and created a favorable environment for CTL immuno-response. Overall, this study revealed a remarkable feature of PLGA NP as delivery platform for immune cells in the tumor microenvironment, which rendered it a powerful tool for re-engineering tumor immune microenvironment for boosting immune therapy.

Supplementary Material

Refer to Web version on PubMed Central for supplementary material.

Acknowledgments

The authors graciously thank NIH for funding (grants CA149363, CA149387, CA151652 and DK100664). We thank Yi Zhao, Lei Miao and Shutao Guo for their technical assistance in the experiment and Andrew Mackenzie Blair for his assistance in manuscript preparation.

References

1. Denies S, Cicchelero L, Van Audenhove I, Sanders NN. Combination of interleukin-12 gene therapy, metronomic cyclophosphamide and DNA cancer vaccination directs all arms of the immune system towards tumor eradication. Journal Of Controlled Release. 2014; 187:175–182. [PubMed: 24887014]
2. Tan Z, Zhou J, Cheung AK, Yu Z, Cheung KW, Liang J, et al. Vaccine-Elicited CD8+ T Cells Cure Mesothelioma by Overcoming Tumor-Induced Immunosuppressive Environment. Cancer research. 2014; 74:6010–6021. [PubMed: 25125656]
3. Venanzi F, Shifrin V, Sherman M, Gabai V, Kiselev O, Komissarov A, et al. Broad-spectrum anti-tumor and anti-metastatic DNA vaccine based on p62-encoding vector. Oncotarget. 2013; 4:1829–1835. [PubMed: 24121124]
4. Schwartzentruber DJ, Lawson DH, Richards JM, Conry RM, Miller DM, Treisman J, et al. gp100 peptide vaccine and interleukin-2 in patients with advanced melanoma. N Engl J Med. 2011; 364:2119–2127. [PubMed: 21631324]
5. Slingluff CL Jr, Petroni GR, Chianese-Bullock KA, Smolkin ME, Ross MI, Haas NB, et al. Randomized multicenter trial of the effects of melanoma-associated helper peptides and cyclophosphamide on the immunogenicity of a multipeptide melanoma vaccine. J Clin Oncol. 2011; 29:2924–2932. [PubMed: 21690475]
6. Weber JS, Kudchadkar RR, Yu B, Gallenstein D, Horak CE, Inzunza HD, et al. Safety, efficacy, and biomarkers of nivolumab with vaccine in ipilimumab-refractory or -naive melanoma. J Clin Oncol. 2013; 31:4311–4318. [PubMed: 24145345]
7. Mellman I, Coukos G, Dranoff G. Cancer immunotherapy comes of age. Nature. 2011; 480:480–489. [PubMed: 22193102]
8. Sharma P, Wagner K, Wolchok JD, Allison JP. Novel cancer immunotherapy agents with survival benefit: recent successes and next steps. Nat Rev Cancer. 2011; 11:805–812. [PubMed: 22020206]
9. Buhrman JD, Slansky JE. Improving T cell responses to modified peptides in tumor vaccines. Immunol Res. 2013; 55:34–47. [PubMed: 22936035]
10. Devaud C, John LB, Westwood JA, Darcy PK, Kershaw MH. Immune modulation of the tumor microenvironment for enhancing cancer immunotherapy. Oncoimmunology. 2013; 2:e25961. [PubMed: 24083084]
11. Xu Z, Ramishetti S, Tseng YC, Guo S, Wang Y, Huang L. Multifunctional nanoparticles co-delivering Trp2 peptide and CpG adjuvant induce potent cytotoxic T-lymphocyte response against melanoma and its lung metastasis. Journal of controlled release : official journal of the Controlled Release Society. 2013; 172:259–265. [PubMed: 24004885]

12. Xu Z, Wang Y, Zhang L, Huang L. Nanoparticle-delivered transforming growth factor-beta siRNA enhances vaccination against advanced melanoma by modifying tumor microenvironment. ACS nano. 2014; 8:3636–3645. [PubMed: 24580381]
13. Chen CA, Ho CM, Chang MC, Sun WZ, Chen YL, Chiang YC, et al. Metronomic chemotherapy enhances antitumor effects of cancer vaccine by depleting regulatory T lymphocytes and inhibiting tumor angiogenesis. Molecular therapy : the journal of the American Society of Gene Therapy. 2010; 18:1233–1243. [PubMed: 20372107]
14. Emens LA, Asquith JM, Leatherman JM, Kobrin BJ, Petrik S, Laiko M, et al. Timed sequential treatment with cyclophosphamide, doxorubicin, and an allogeneic granulocyte-macrophage colony-stimulating factor-secreting breast tumor vaccine: a chemotherapy dose-ranging factorial study of safety and immune activation. J Clin Oncol. 2009; 27:5911–5918. [PubMed: 19805669]
15. Gameiro SR, Caballero JA, Higgins JP, Apelian D, Hodge JW. Exploitation of differential homeostatic proliferation of T-cell subsets following chemotherapy to enhance the efficacy of vaccine-mediated antitumor responses. Cancer Immunol Immunother. 2011; 60:1227–1242. [PubMed: 21544650]
16. Neninger E, Verdecia BG, Crombet T, Viada C, Pereda S, Leonard I, et al. Combining an EGF-based cancer vaccine with chemotherapy in advanced nonsmall cell lung cancer. Journal of immunotherapy. 2009; 32:92–99. [PubMed: 19307998]
17. Liby KT, Sporn MB. Synthetic oleanane triterpenoids: multifunctional drugs with a broad range of applications for prevention and treatment of chronic disease. Pharmacol Rev. 2012; 64:972–1003. [PubMed: 22966038]
18. Wang YY, Zhe H, Zhao R. Preclinical evidences toward the use of triterpenoid CDDO-Me for solid cancer prevention and treatment. Mol Cancer. 2014; 13:30. [PubMed: 24552536]
19. Deeb D, Gao X, Jiang H, Dulchavsky SA, Gautam SC. Oleanane triterpenoid CDDO-Me inhibits growth and induces apoptosis in prostate cancer cells by independently targeting pro-survival Akt and mTOR. Prostate. 2009; 69:851–860. [PubMed: 19189297]
20. Liu YB, Gao XH, Deeb D, Gautam SC. Oleanane triterpenoid CDDO-Me inhibits Akt activity without affecting PDK1 kinase or PP2A phosphatase activity in cancer cells. Biochemical And Biophysical Research Communications. 2012; 417:570–575. [PubMed: 22177954]
21. Qin Y, Deng W, Ekmekcioglu S, Grimm EA. Identification of unique sensitizing targets for anti-inflammatory CDDO-Me in metastatic melanoma by a large-scale synthetic lethal RNAi screening. Pigment Cell Melanoma Res. 2013; 26:97–112. [PubMed: 23020131]
22. Ryu K, Susa M, Choy E, Yang C, Hornicek FJ, Mankin HJ, et al. Oleanane triterpenoid CDDO-Me induces apoptosis in multidrug resistant osteosarcoma cells through inhibition of Stat3 pathway. Bmc Cancer. 2010:10. [PubMed: 20064265]
23. Deeb D, Gao X, Arbab AS, Barton K, Dulchavsky SA, Gautam SC. CDDO-Me: A Novel Synthetic Triterpenoid for the Treatment of Pancreatic Cancer. Cancers. 2010; 2:1779–1793. [PubMed: 21799944]
24. Gao X, Liu Y, Deeb D, Liu P, Liu A, Arbab AS, et al. ROS mediate proapoptotic and antisurvival activity of oleanane triterpenoid CDDO-Me in ovarian cancer cells. Anticancer Res. 2013; 33:215–221. [PubMed: 23267148]
25. Shishodia S, Sethi G, Konopleva M, Andreeff M, Aggarwal BB. A synthetic triterpenoid, CDDO-Me, inhibits I kappa B alpha, kinase and enhances apoptosis induced by TNF and chemotherapeutic agents through down-regulation of expression of nuclear factor kappa B-regulated gene products in human leukemic cells. Clinical Cancer Research. 2006; 12:1828–1838. [PubMed: 16551868]
26. Nagaraj S, Youn JI, Weber H, Iclozan C, Lu L, Cotter MJ, et al. Anti-inflammatory triterpenoid blocks immune suppressive function of MDSCs and improves immune response in cancer. Clinical cancer research : an official journal of the American Association for Cancer Research. 2010; 16:1812–1823. [PubMed: 20215551]
27. Liao D, Liu Z, Wrasidlo WJ, Luo Y, Nguyen G, Chen T, et al. Targeted therapeutic remodeling of the tumor microenvironment improves an HER-2 DNA vaccine and prevents recurrence in a murine breast cancer model. Cancer research. 2011; 71:5688–5696. [PubMed: 21784871]

28. Hu Y, Haynes MT, Wang Y, Liu F, Huang L. A highly efficient synthetic vector: nonhydrodynamic delivery of DNA to hepatocyte nuclei in vivo. ACS nano. 2013; 7:5376–5384. [PubMed: 23647441]
29. Li J, Yang Y, Huang L. Calcium phosphate nanoparticles with an asymmetric lipid bilayer coating for siRNA delivery to the tumor. Journal of controlled release : official journal of the Controlled Release Society. 2012; 158:108–114. [PubMed: 22056915]
30. Zhang Y, Peng L, Mumper RJ, Huang L. Combinational delivery of c-myc siRNA and nucleoside analogs in a single, synthetic nanocarrier for targeted cancer therapy. Biomaterials. 2013; 34:8459–8468. [PubMed: 23932296]
31. Zhang Y, Schwerbrock NM, Rogers AB, Kim WY, Huang L. Codelivery of VEGF siRNA and gemcitabine monophosphate in a single nanoparticle formulation for effective treatment of NSCLC. Molecular therapy : the journal of the American Society of Gene Therapy. 2013; 21:1559–1569. [PubMed: 23774791]
32. Ishida E, Managit C, Kawakami S, Nishikawa M, Yamashita F, Hashida M. Biodistribution characteristics of galactosylated emulsions and incorporated probucol for hepatocyte-selective targeting of lipophilic drugs in mice. Pharmaceutical research. 2004; 21:932–939. [PubMed: 15212156]
33. Obermajer N, Wong JL, Edwards RP, Odunsi K, Moysich K, Kalinski P. PGE(2)-driven induction and maintenance of cancer-associated myeloid-derived suppressor cells. Immunological investigations. 2012; 41:635–657. [PubMed: 23017139]
34. Shirota Y, Shirota H, Klinman DM. Intratumoral injection of CpG oligonucleotides induces the differentiation and reduces the immunosuppressive activity of myeloid-derived suppressor cells. Journal of immunology. 2012; 188:1592–1599.
35. Sinha P, Clements VK, Ostrand-Rosenberg S. Interleukin-13-regulated M2 macrophages in combination with myeloid suppressor cells block immune surveillance against metastasis. Cancer research. 2005; 65:11743–11751. [PubMed: 16357187]
36. Wu A, Wei J, Kong LY, Wang Y, Priebe W, Qiao W, et al. Glioma cancer stem cells induce immunosuppressive macrophages/microglia. Neuro-oncology. 2010; 12:1113–1125. [PubMed: 20667896]
37. Kashimura S, Saze Z, Terashima M, Soeta N, Ohtani S, Osuka F, et al. CD83(+) dendritic cells and Foxp3(+) regulatory T cells in primary lesions and regional lymph nodes are inversely correlated with prognosis of gastric cancer. Gastric cancer : official journal of the International Gastric Cancer Association and the Japanese Gastric Cancer Association. 2012; 15:144–153.
38. Kim S, Lee A, Lim W, Park S, Cho MS, Koo H, et al. Zonal difference and prognostic significance of foxp3 regulatory T cell infiltration in breast cancer. Journal of breast cancer. 2014; 17:8–17. [PubMed: 24744792]
39. Mattarollo SR, Steegh K, Li M, Duret H, Foong Ngiow S, Smyth MJ. Transient Foxp3(+) regulatory T-cell depletion enhances therapeutic anticancer vaccination targeting the immune-stimulatory properties of NKT cells. Immunology and cell biology. 2013; 91:105–114. [PubMed: 23090488]
40. Diaz-Montero CM, Finke J, Montero AJ. Myeloid-derived suppressor cells in cancer: therapeutic, predictive, and prognostic implications. Seminars in oncology. 2014; 41:174–184. [PubMed: 24787291]
41. Weed DT, Vella JL, Reis IM, De la Fuente AC, Gomez C, Sargi Z, et al. Tadalafil reduces myeloid-derived suppressor cells and regulatory T cells and promotes tumor immunity in patients with head and neck squamous cell carcinoma. Clinical cancer research : an official journal of the American Association for Cancer Research. 2015; 21:39–48. [PubMed: 25320361]
42. Wallecha A, Singh R, Malinina I. Listeria monocytogenes (Lm)-LLO immunotherapies reduce the immunosuppressive activity of myeloid-derived suppressor cells and regulatory T cells in the tumor microenvironment. Journal of immunotherapy. 2013; 36:468–476. [PubMed: 24145358]
43. Alizadeh D, Larmonier N. Chemotherapeutic targeting of cancer-induced immunosuppressive cells. Cancer research. 2014; 74:2663–2668. [PubMed: 24778417]

44. Ostrand-Rosenberg S, Sinha P, Beury DW, Clements VK. Cross-talk between myeloid-derived suppressor cells (MDSC), macrophages, and dendritic cells enhances tumor-induced immune suppression. Seminars in cancer biology. 2012; 22:275–281. [PubMed: 22313874]
45. Whiteside TL. The tumor microenvironment and its role in promoting tumor growth. Oncogene. 2008; 27:5904–5912. [PubMed: 18836471]
46. Kuriyan AE, Lehmann GM, Kulkarni AA, Woeller CF, Feldon SE, Hindman HB, et al. Electrophilic PPARgamma ligands inhibit corneal fibroblast to myofibroblast differentiation in vitro: a potentially novel therapy for corneal scarring. Exp Eye Res. 2012; 94:136–145. [PubMed: 22178289]
47. Guo ST, Lin CM, Xu ZH, Miao L, Wang YH, Huang L. Co-delivery of Cisplatin and Rapamycin for Enhanced Anticancer Therapy through Synergistic Effects and Microenvironment Modulation. ACS nano. 2014; 8:4996–5009. [PubMed: 24720540]
48. Zhang J, Miao L, Guo S, Zhang Y, Zhang L, Satterlee A, et al. Synergistic anti-tumor effects of combined gemcitabine and cisplatin nanoparticles in a stroma-rich bladder carcinoma model. Journal of controlled release : official journal of the Controlled Release Society. 2014; 182:90–96. [PubMed: 24637468]
49. Johansson A, Ganss R. Remodeling of tumor stroma and response to therapy. Cancers. 2012; 4:340–353. [PubMed: 24213314]
50. Matejuk A, Collet G, Nadim M, Grillon C, Kieda C. MicroRNAs and tumor vasculature normalization: impact on anti-tumor immune response. Archivum immunologiae et therapiae experimentalis. 2013; 61:285–299. [PubMed: 23575964]
51. Konkankit VV, Kim W, Koya RC, Eskin A, Dam MA, Nelson S, et al. Decitabine immunosensitizes human gliomas to NY-ESO-1 specific T lymphocyte targeting through the Fas/Fas ligand pathway. Journal of translational medicine. 2011; 9:192. [PubMed: 22060015]
52. Solary E, Micheau O, Dimanche-Boitrel MT, Martin F. [The Fas/Fas-ligand system: implications in the antitumor immune response and in the activity of cytotoxic agents]. Bull Cancer. 1998; 85:685–694. [PubMed: 9754077]
53. Viard-Leveugle I, Gaide O, Jankovic D, Feldmeyer L, Kerl K, Pickard C, et al. TNF-alpha and IFN-gamma are potential inducers of Fas-mediated keratinocyte apoptosis through activation of inducible nitric oxide synthase in toxic epidermal necrolysis. The Journal of investigative dermatology. 2013; 133:489–498. [PubMed: 22992806]

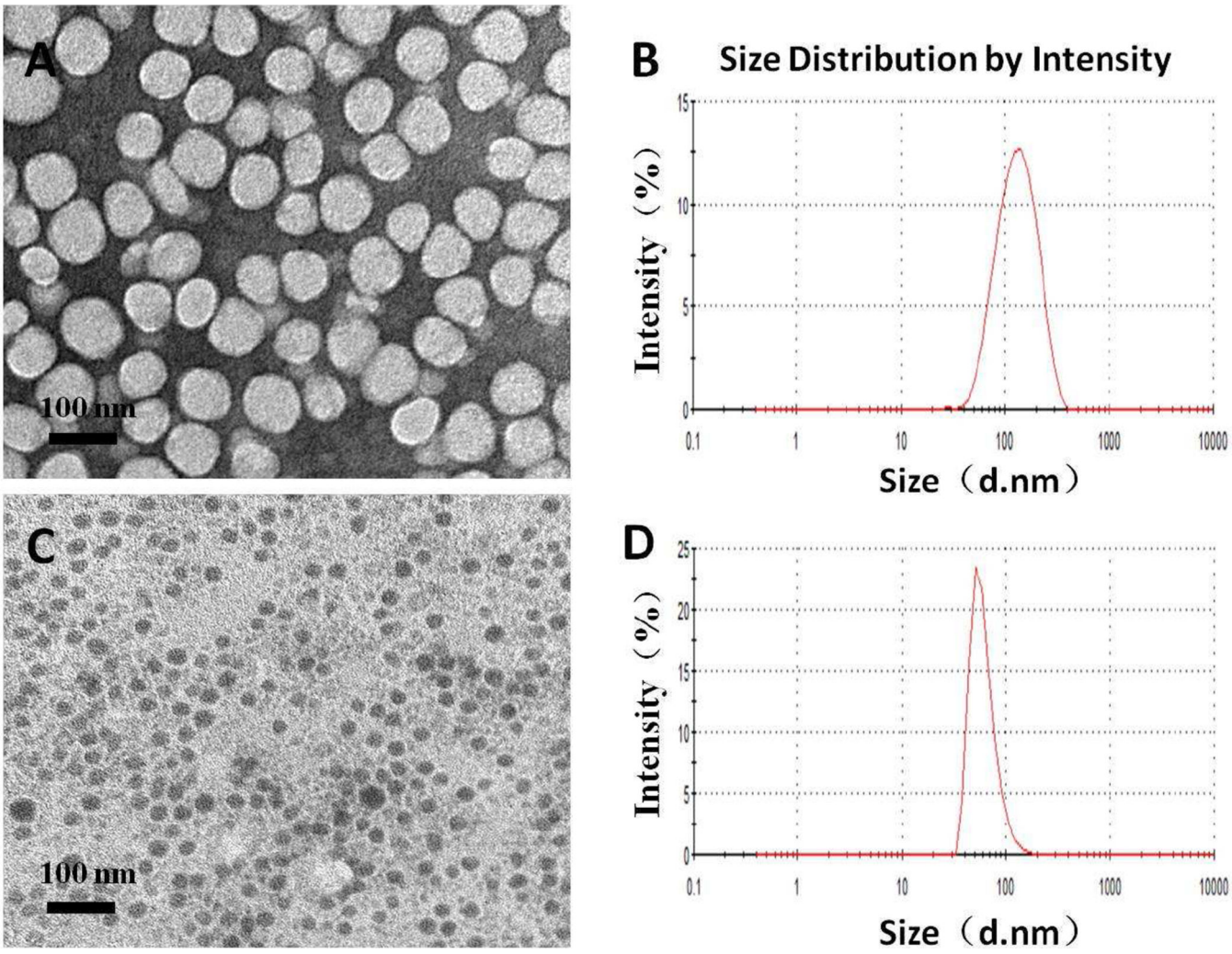

Figure 1.

Physicochemical characterization of CDDO-Me NP and p-Trp2 LCP NP. TEM images of CDDO-Me NP (A) after negative staining and p-Trp2 LCP NP (C). DLS size distribution of CDDO-Me NP (B) and p-Trp2 LCP NP (D).

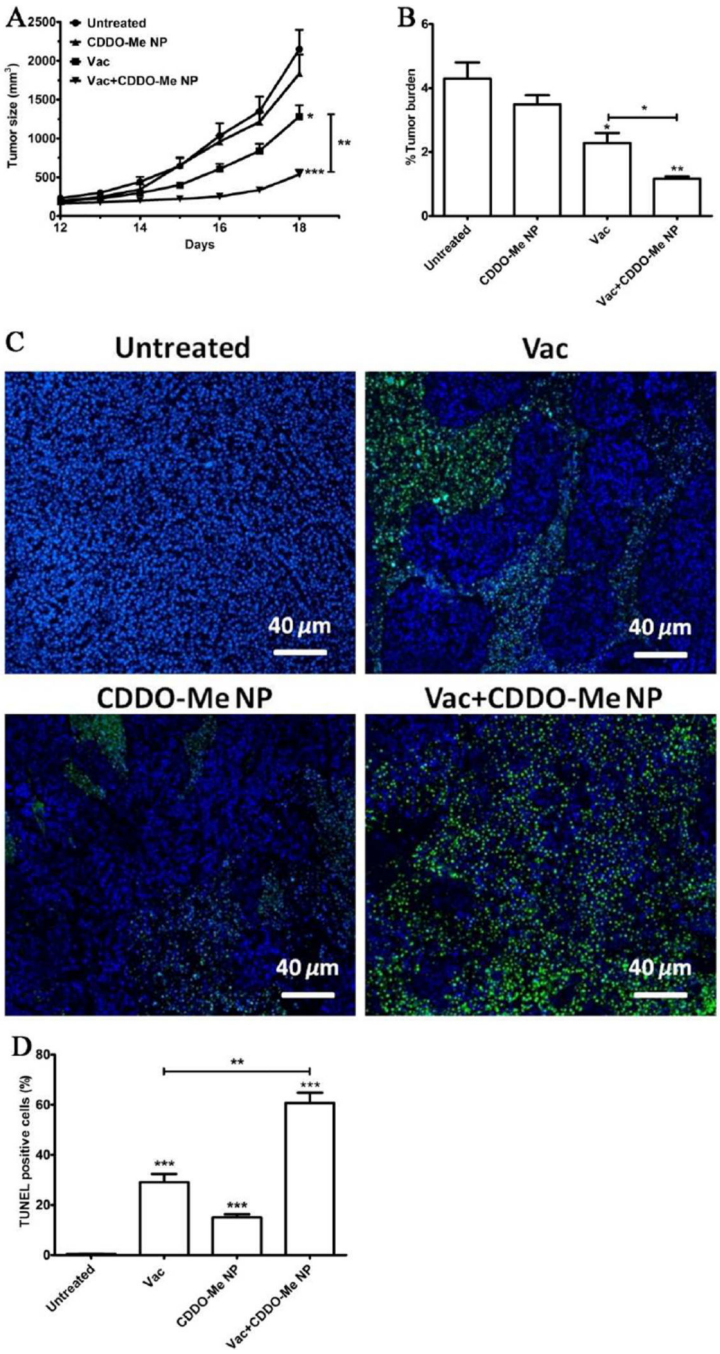

Figure 2.

Antitumor activity and apoptosis assay of Vac, CDDO-Me NP and Vac+CDDO-Me NP on B16F10 tumor bearing mice. C57BL/6 mice were inoculated with 2×10^5 B16F10 cells on day 0. Vac was injected on day 13 at a dose of 0.3 mg/kg; CDDO-Me NP was administered on days 13, 15 and 17 at a dose of 5 mg/kg. Tumor growth was measured every day for 18 days. Mice were sacrificed on day 18 and tumors were harvested. Tumor growth (A) and tumor burden (B) were measured. Clusters of TUNEL-positive nuclei (green fluorescence) were observed in the tumor treated with Vac. Dispersed TUNEL-positive nuclei were

observed in CDDO-Me NP. Extensive TUNEL-positive nuclei were observed in the Vac +CDDO-Me NP group (C). Three randomly selected microscopic fields were quantitatively analyzed using Image J. The results are displayed as mean ± SEM (error bars) (D). Statistical analyses were done by comparing with the untreated unless specified with markings.*$p < 0.05$, **$p < 0.01$, ***$p < 0.001$, $n = 5$.

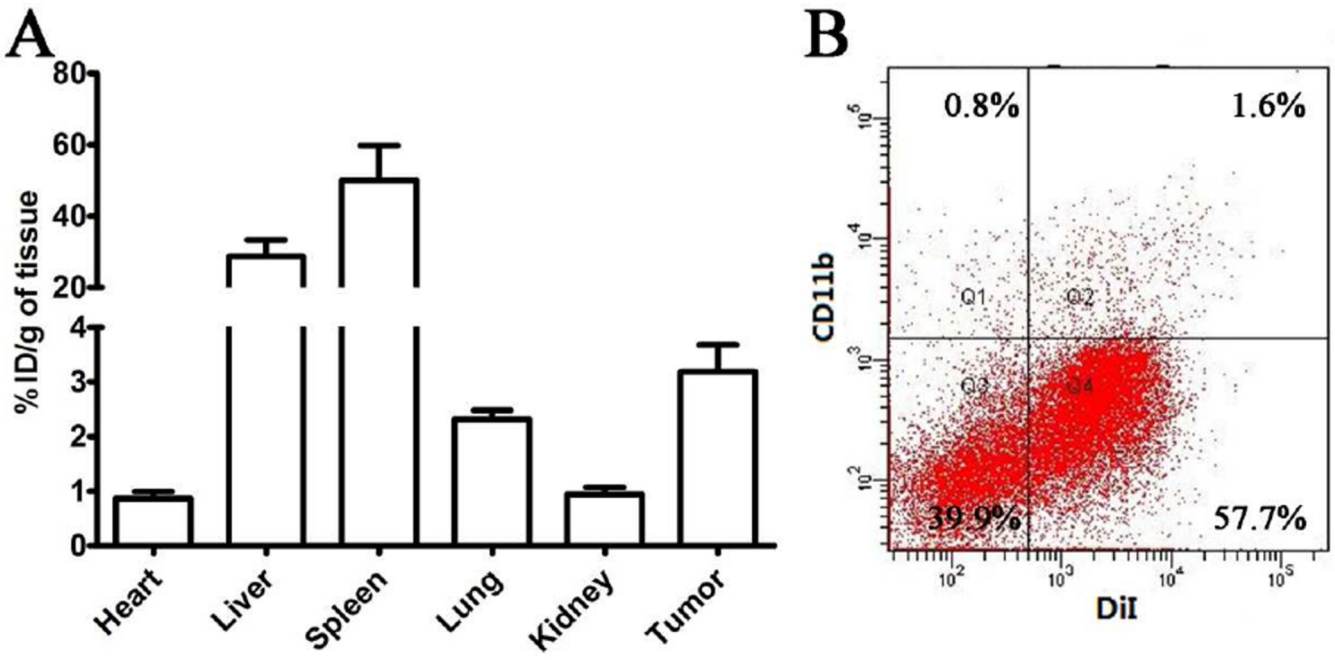

Figure 3.

^{3}H-labeled PLGA NP biodistribution showed a high accumulation in B16F10 tumor tissue in tumor bearing mice in 24 h (A). Subcellular uptake of DiI-labeled PLGA NP in tumor cells including the CD11b+ immunocyte at 24 h post injection (B).

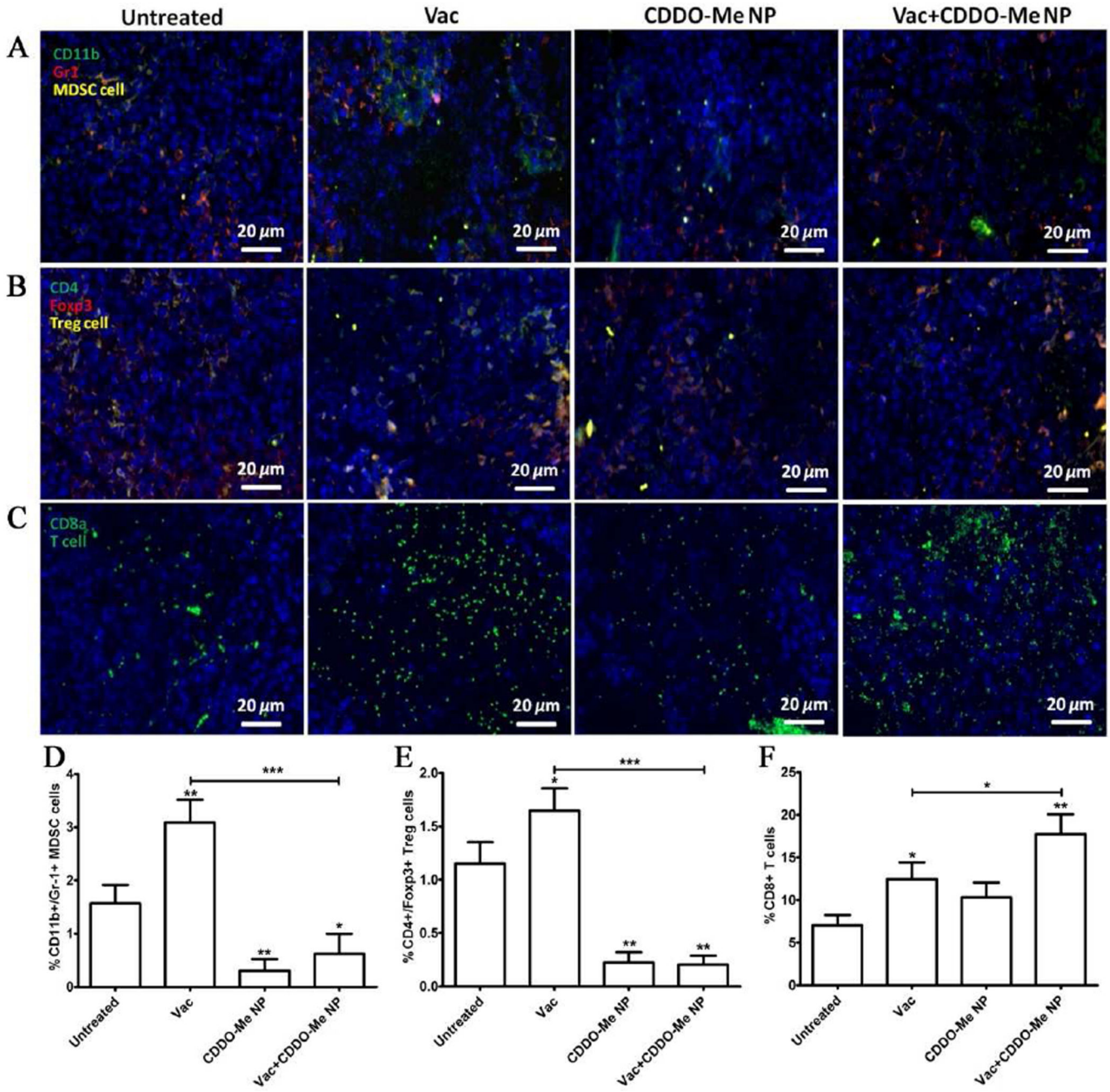

Figure 4.

Tumor infiltrates immune cells after treatment. C57BL/6 mice were inoculated with 2×10^5 B16F10 cells on day 0. Vac was injected on day 13 at a dose of 0.3 mg/kg; CDDO-Me NP was administered on days 13, 15 and 17 at a dose of 5 mg/kg. Mice were sacrificed on day 18 and tumors were harvested. Tumor tissues were assayed for CD8+ T cells, Treg cells and MDSC cells with immunofluorescence staining (A, B, C) or flow cytometry (D, E, F) analysis. The results are displayed as mean ± SEM (error bars). Statistical analyses were done by comparing to the untreated unless otherwise specified with markings.*$p < 0.05$, **$p < 0.01$, ***$p < 0.001$, $n = 5$.

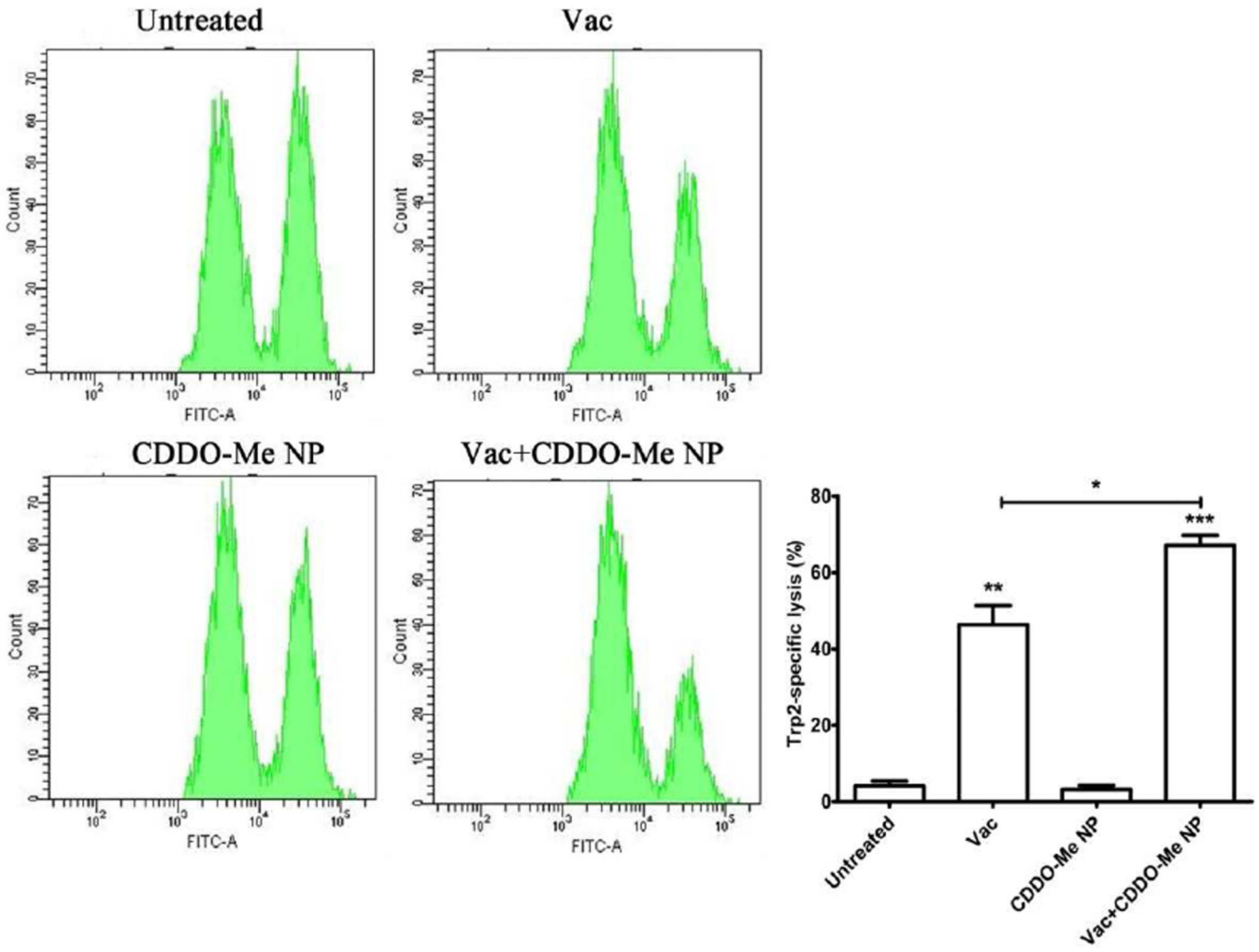

Figure 5.

In vivo CTL response after vaccination under various conditions. C57BL/6 mice were subcutaneously injected with Vac on day 1, and injected with CDDO-Me NP on days 1, 3 and 5. Splenocytes from naïve mice were pulsed with Ova or Trp2 peptide and stained with low (Ova) or high (Trp2) concentrations of CFSE, respectively. The cells were then mixed and injected into the vaccinated mice. After 18 h, splenocytes from the vaccinated mice were analyzed by flow cytometry and enumerated according to a published equation. Representative graph from each group is shown. *$p < 0.05$, **$p < 0.01$, ***$p < 0.001$, $n = 5$.

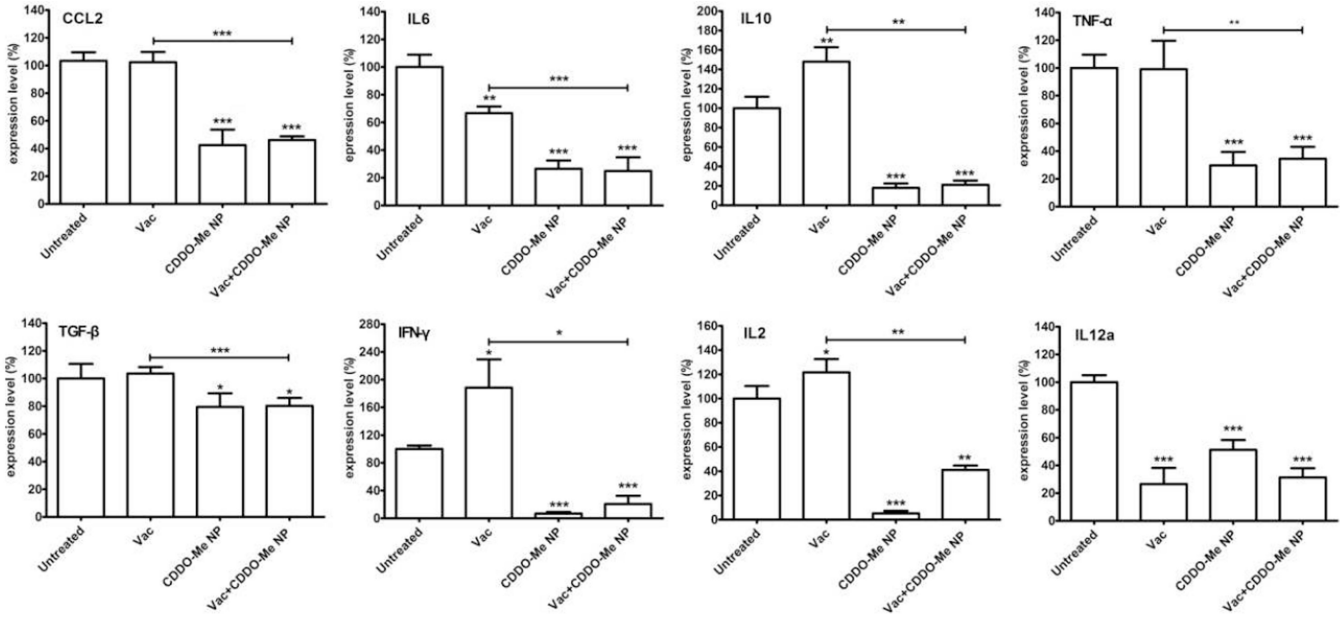

Figure 6.

Tumor local cytokine levels after vaccination. C57BL/6 mice were inoculated with 2×10^5 B16F10 cells on day 0. The Vac was given on day 13 and CDDO-Me NP were given on days 13, 15 and 17. Mice were sacrificed on day 18, and tumors were collected for cytokine detection using RT-PCR. The results are displayed as mean ± SEM (error bars). Statistical analyses were done by comparison with the untreated. *$p < 0.05$, **$p < 0.01$, *** $p < 0.001$, $n = 5$.

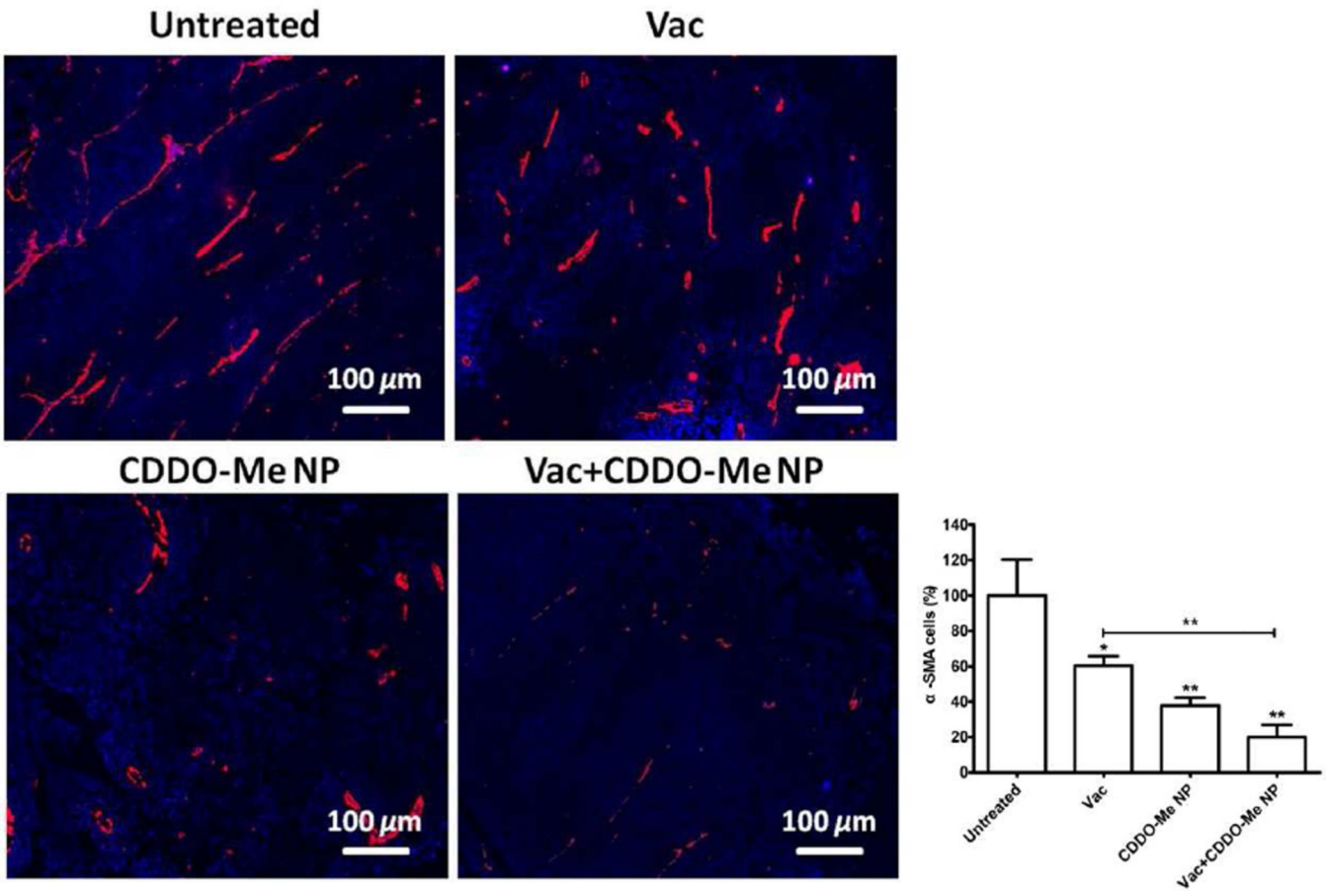

Figure 7.

TAF in B16F10 tumors were stained with α-SMA antibody (red), the percentage denotes the average percentage of α-SMA+ fibroblasts (red). Three randomly selected microscopic fields were quantitatively analyzed using Image J. The results are displayed as mean ± SEM (error bars). Statistical analyses were done by comparing to the untreated unless specified with markings.*$p < 0.05$, **$p < 0.01$, $n = 3$.

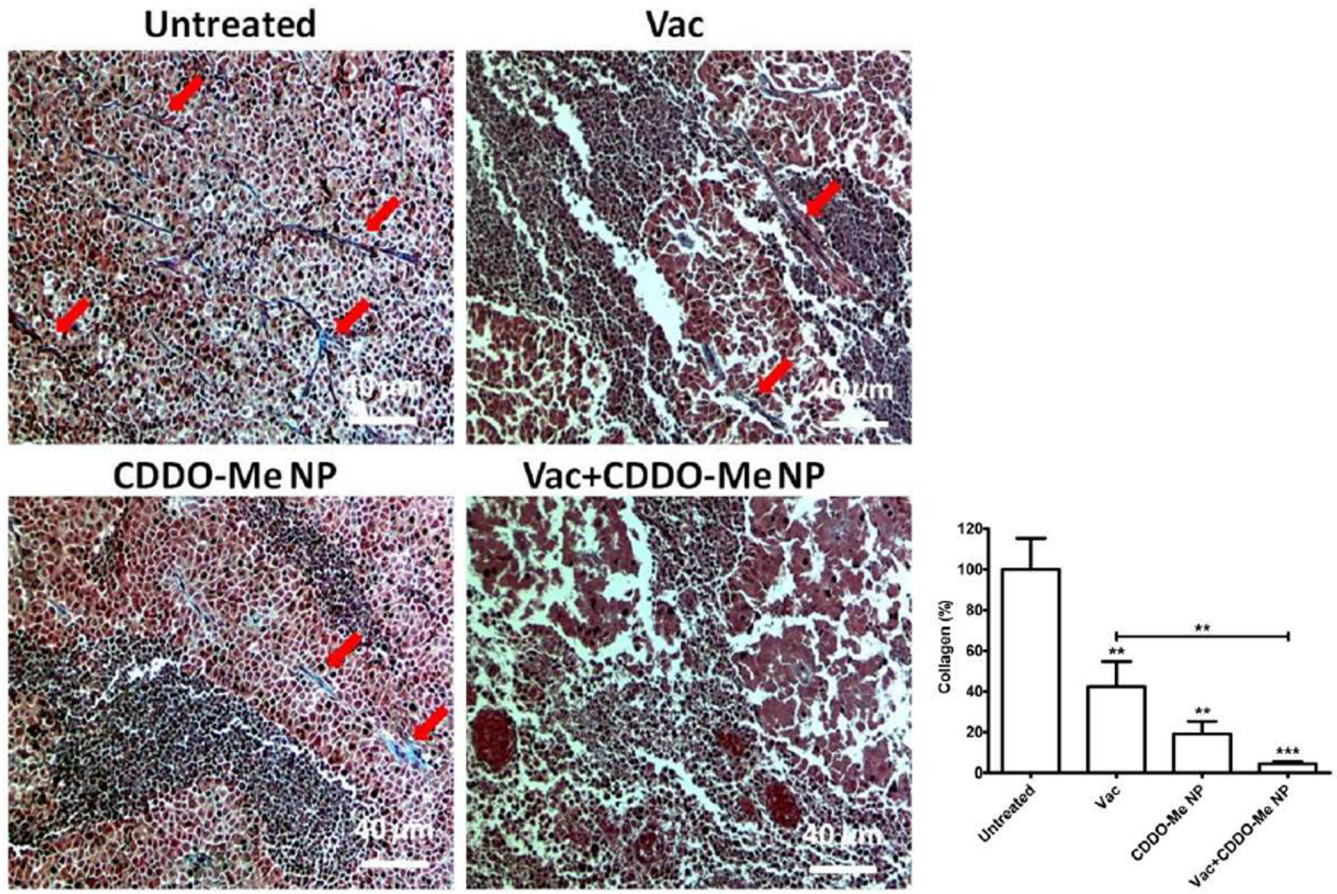

Figure 8.

Tumor sections were stained with Masson Trichrome. The blue color represents collagen fibers (red arrows). Three randomly selected microscopic fields were quantitatively analyzed using Image J. The results are displayed as mean ± SEM (error bars). Statistical analyses were done by comparing to the untreated unless specified with markings. $^{**}p < 0.01$, $^{***}p < 0.001$, $n = 3$.

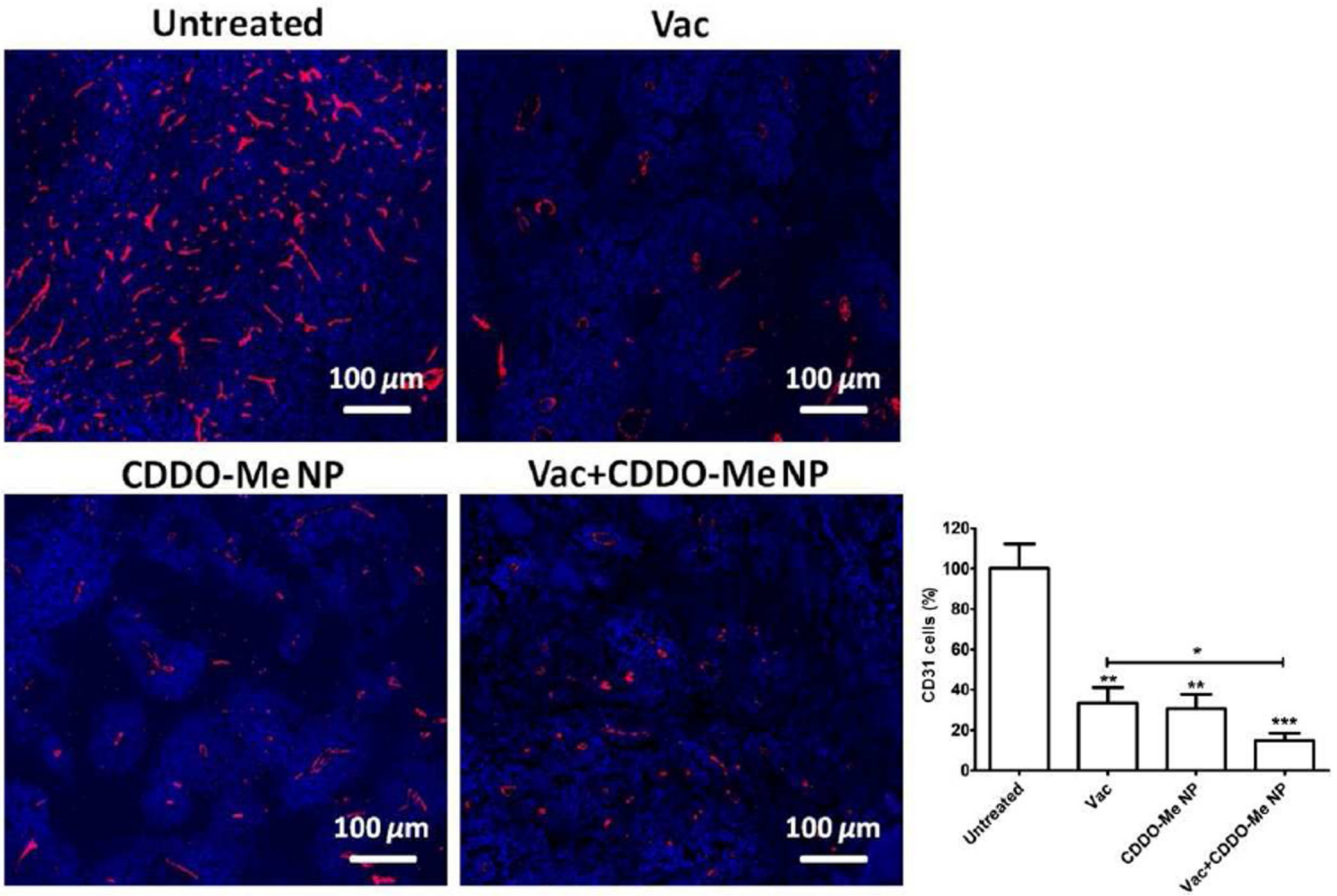

Figure 9.

Vessels in B16F10 tumor were stained with CD31 antibody (red), the percentage denotes the average percentage of CD31+ vessels. Three randomly selected microscopic fields were quantitatively analyzed using Image J. The results are displayed as mean ± SEM (error bars). Statistical analyses were done by comparing to the untreated unless specified with markings.*$p < 0.05$, **$p < 0.01$, ***$p < 0.001$, $n = 3$.

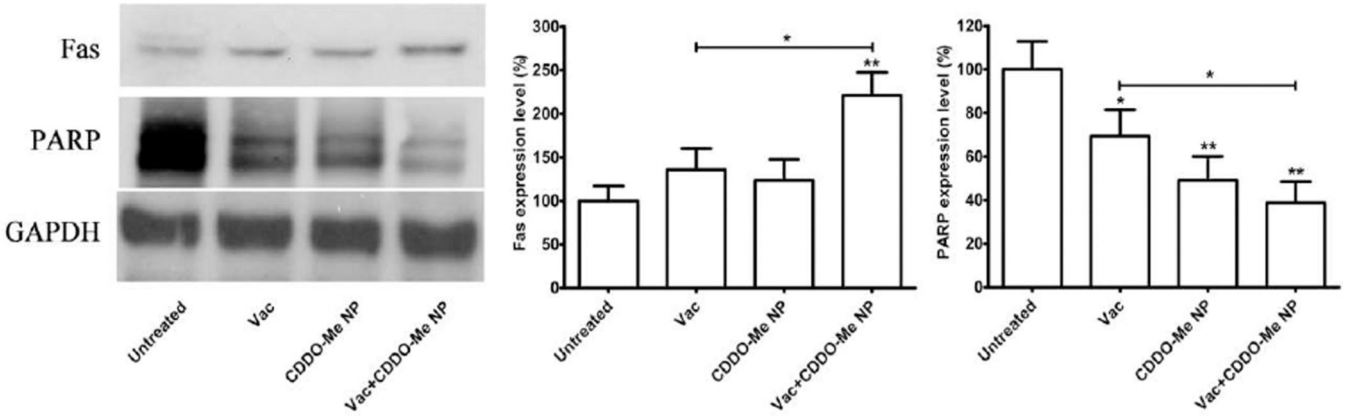

Figure 10.

Expression levels of Fas and PARP in tumor samples after treatments. C57BL/6 mice were inoculated with 2×10^5 B16F10 cells on day 0. Vac was injected on day 13 at a dose of 0.3 mg/kg; CDDO-Me NP was administered on days 13, 15 and 17 at a dose of 5 mg/kg. Mice were sacrificed on day 18 and tumors were collected for western blot analysis. The results are displayed as mean ± SEM (error bars). Statistical analyses were done by comparing with the untreated unless specified with markings.*$p < 0.05$, **$p < 0.01$, $n = 3$.

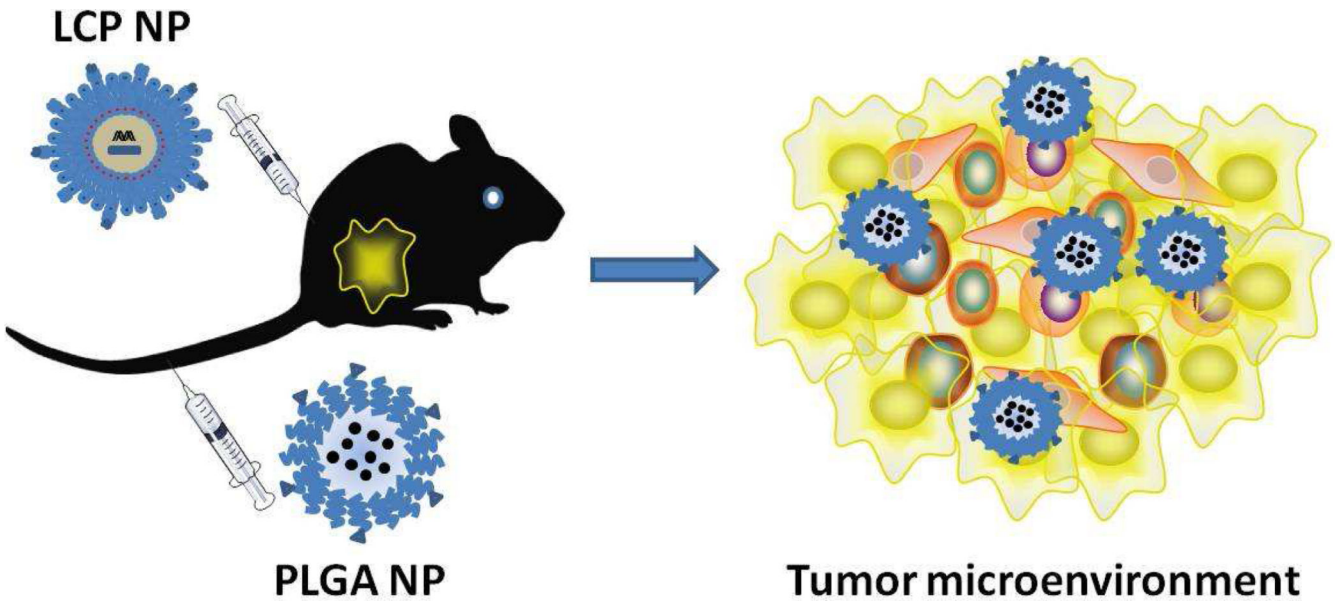

Scheme 1.

Schematic illustration of PLGA-based CDDO-Me NP and LCP-based p-Trp2 vaccine NP inject to the mouse.

TABLE 1

Primer	Applied Biosystems/ref
Mouse TGF-β1	Mm01178820_m1
Mouse IL6	Mm00446190_m1
Mouse TNF-α	Mm00443260_g1
Mouse CCL2	Mm00441242_m1
Mouse IFN-γ	Mm01 168134_m1
Mouse IL10	Mm00439614_m1
Mouse IL12a	Mm00434165_m1
Mouse IL2	Mm00434256_m1
Mouse GAPDH	Mm99999915_g1